Technical University of Denmark

Power ramp and fission gas performance of fuel pins M20-1B, M2-2B and T9-3B

Knudsen, P.; Bagger, Carsten

Publication date:
1978

Document Version
Publisher's PDF, also known as Version of record

Citation (APA):
Knudsen, P., & Bagger, C. (1978). Power ramp and fission gas performance of fuel pins M20-1B, M2-2B and T9-3B. (Risø-M; No. 2151).

A. E. K. Risø

Risø-M-2151

Risø-M-

Title and author(s)

POWER RAMP AND FISSION GAS PERFORMANCE OF FUEL PINS M20-1B, M2-2B AND T9-3B

by

P. Knudsen and C. Bagger

16 pages + 10 tables + 6 illustrations

Date December 1978

Department or group

Metallurgy

Group's own registration number(s)

Abstract

Three UO_2-Zr test fuel pins were irradiated together to 2330 GJ/kg U (23,800 MWD/te UO_2) at heat loads decreasing from 50 to 24 kW/m (500 to 240 W/cm) (test average levels), the latest being 31 kW/m (310 W/cm). One pin was then power ramped to 45 kW/m (450 W/cm) at 35 W/m.s (21 W/cm.min.) and kept there for 2 Ms (550 hrs.) without failure indication.

The other two pins were further irradiated to 2450 GJ/kg U (25,000 MWD/te UO_2) at approximately 23 kW/m (230 W/cm). Ramp testing to 43 kW/m (430 W/cm) did not produce failure during 2.4 Ms (670 hrs.).

The fission gas release in the three pins was 30-40%. A limited metallographic examination revealed extensive fuel-clad reaction.

Design and irradiation details are included for use as input in the validation of fuel performance codes.

Copies to

Available on request from the Library of the Danish Atomic Energy Commission (Atomenergikommissionens Bibliotek), Risø, DK-4000 Roskilde, Denmark
Telephone: (03) 35 51 01, ext. 334, telex: 43116

ISBN 87-550-0571-3

LIST OF CONTENTS

POWER RAMP AND FISSION GAS PERFORMANCE OF FUEL PINS M20-1B, M2-2B AND T9-3B

by

P. Knudsen and C. Bagger

INTRODUCTION

Rapid power increases may lead to failure of irradiated UO_2-Zr fuel pins, and experience is being accumulated from power reactor operation as well as test reactor experiments with carefully controlled operating conditions. Published results on power ramp performance were, however, generally obtained at burnup levels around 1960 GJ/kg U (20,000 MWD/te UO_2) or less. With the present interest in achieving an improved fuel utilization, it is desirable to extend the lifetime of water reactor fuel. There is, consequently, a need for experimental data on power ramp performance at increasing burnup levels.

The Danish ramp test programme includes experiments at significant burnups (e.g. Refs. (1) and (2). This paper presents further results which were obtained with three BWR-type test fuel pins ramp tested at 2500 and 2450 GJ/kg U (25,500 and 25,000 MWD/te UO_2). Details are given so that the data can be used in the validation of fuel performance codes. This applies to general ramp performance as well as fission gas release, since all three pins remained intact during the overpower application.

FUEL PIN DESIGN

The three almost identical test fuel pins had 12.6 mm sintered UO_2 pellets of 1.45% enrichment (end pellets with natural ^{235}U

content) in approximately 126 mm long stacks. The cladding was cold-worked and stress-relieved Zr-2 or Zr-4 tubing of 0.55 mm wall thickness which had been autoclaved on both sides. The mechanical properties were nearly the same for the two cladding materials. The diametral pellet-clad clearance was 0.21-0.24 mm, and the pins were backfilled with 0.1 MPa He (1 ata He). Further design details are given in Table I.

IRRADIATION

Facility

Each irradiation was performed in a water-cooled rig (see Refs. (3) and (4)) in the 10 MW heavy-water materials testing reactor DR 3 at Risø. The normal reactor cycle comprises 2 Ms (23½ days) at full reactor power, 0.4 Ms (4½ days) shut-down for exchange of experiments and maintenance.

The irradiation rig was loaded in a hollow, highly enriched U-Al driver fuel element in a core position corresponding to the desired heat load. In this rig type, the fuel pin is cooled by natural convection inside the rig of the primary water (H_2O) pressurized to 7.2 MPa (70 ato) with He gas. There is a small external circulation of the primary water for purification purposes. A gamma monitor is placed near the rig outlet and serves as indicator for fuel pin failure. The flow time from the fuel pin to the monitor position is estimated to be about 360 s. The rig thermal output is determined from flow rate and temperature increase of the secondary cooling water.

Conditions

The thermal output from a test (i.e. one or several fuel pins screwed together axially) was obtained by correcting the rig thermal output for gamma heat generation. Lineat heat load and burnup levels were then calculated as test average values, distributing the heat output locally according to the initial enrichments of central and end pellets of the fuel pin(s) composing the test. A summary of the power histories obtained in this way was presented elsewhere (5).

Gamma scans on several fission products indicated that the fission density of the (initially lower enriched) end pellets had increased during the irradiation and approached the level of the central pellets. This is a results of different Pu build-up rates caused by different initial ^{235}U contents and correspondingly different neutron captures. Gamma scans of these and similar irradiations have also revealed a certain peaking effect near the pellet stack ends. However, this usually applies to part of an end pellet only; it is thus considered an effect separate from the difference in Pu build-up rates. The above procedure for calculating linear heat load and burnup is, on this background, only acceptable in the early part of the irradiation period.

Scans on fission product isotopes of various halflives, ranging from ^{137}Cs: 0.97 Gs (30 years) to $^{140}Ba/La$: 1.12 Ms (13 days), were, therefore, evaluated and supplemented with physics calculations. From this, corrected heat load and burnup levels were obtained, as described in the appendix. The data reported in the next section are such corrected values, on a test average basis.

The appendix gives further details about the irradiation conditions, including cladding surface temperature and fast flux levels, as well as a comparison between results from radiochemical analysis and burnup levels, calculated as described above.

Irradiation History

Pre-Ramp Irradiation 013: Pins M2-2B, M20-1B, T9-3B

The three pins were screwed together in the sequence given with M2-2B at the top. A burnup of 2330 GJ/kg U (23,800 MWD/te UO_2) was accumulated over 39 reactor periods. The heat load was generally decreasing in the range 50 to 24 kW/m (500 to 240 W/cm), the latest level being 31 kW/m (310 W/cm). Fig. 1 gives an overview of the entire power history for all the pins.

The test was visually inspected at four intermediate reactor shut-downs, where a gradually increasing extent of surface corrosion was observed. Most of the cladding surfaces were covered with a very thin "soot-like" surface deposit, as also seen with other tests in DR 3 (this surface deposit is easily removable, e.g. with a wet paper tissue).

At the end of the irradiation, the test assembly was unloaded and non-destructively examined. Fig. 2 shows two of the gamma scans referred to above. It is possible to distinguish between central and end pellets on the ^{137}Cs scan (half-life 0.97 Gs (30.6 years)), which provides a fission density distribution smoothed over the whole irradiation period. The $^{95}Zr/Nb$ scan (half-life 5.5 Ms (64 days)) is representative of the latter part of the irradiation period and shows virtually no difference between central and end pellets. Both scans reveal the rather flat axial power shape.

Ramp Test 050: Pin M20-1B

The pin was mounted in the same elevation in the reactor as during the irradiation in test 013, with Zr dummy pins replacing M2-2B and T9-3B. Overpower was applied during a normal reactor start-up, with holds at lower reactor power levels for routine calibration. Details of the power ramp are shown in Fig. 3, the ramp rate being 35 W/m.s (21 W/cm.min.) to the final level of 45 kW/m (450 W/cm). Since there was no failure indication after arrival to the overpower level, the pin remained in the reactor for 2 Ms (550 hrs) and was then unloaded for final examination at 2580 GJ/kg U (26,300 MWD/te UO_2).

Re-Pre-Ramp Irradiation 055: Pins M2-2B, T9-3B

Since the ramp test 050 did not produce a failure, it was decided to continue the pre-ramp irradiation of the other two pins, which were re-assembled in the same elevation as in test 013, with a Zr dummy pin replacing M20-1B in the middle position. The average burnup was then increased to 2450 GJ/kg U (25,000 MWD/te UO_2) at reduced heat load in the range 22-24 kW/m (220-240 W/cm), and the pins were again characterised non-destructively.

Ramp Test 067: Pins M2-2B, T9-3B

An overpower level of 43 kW/m (430 W/cm) (the maximum possible in the DR 3 reactor with these fuel pins) was applied as for test 050, with details given in Fig. 3. There was no failure indication, and the pins stayed in the reactor for 2.4 Ms (670 hrs.) and were then unloaded for final examination at 2540 GJ/kg U (25,900 MWD/te UO_2).

HOT-CELL EXAMINATION

The hot-cell examination at the various stages have included the following types of observations:

- visual inspection
- profilometry
- gamma scanning
- neutron radiography
- eddy current testing (ECT)
- piercing and gas analysis
- metallography.

In the following sections, results are summarised from the non-destructive and the initial metallographic examination, and fission gas data are also presented.

Pin M20-1B (Tests 013 and 050)

Cladding

After test 013, M20-1B had various degrees of surface corrosion as can be seen from Fig. 4. There was no significant change in appearance after the 050 irradiation.

In a metallographic cross-section, the major part of the clad OD was covered by a rather uniform oxde layer about 5 µm thick; certain areas had nodules up to 40 µm thick, some of them "grown together". No surface crud layer was seen. Parts of the clad ID were covered with an oxide layer, being smooth towards the clad but irregular towards the fuel, generally with a thickness of 5-10 µm. At some locations, reaction had apparently occurred between clad and fuel.

After the 013-irradiation, the outer diameter had decreased by an average amount of about 50 µm, and ridges up to 25 µm (diametral) could be seen. Test 050 produced minor diameter increases, not exceeding some 20 µm. No ECT results were obtained before the 050 ramp test, owing to unavailability of equipment. Besides ridges, there was nothing of interest on the post-ramp traces. Neutron radiography revealed some signs of slight hydriding of the cladding just above the fuel stack.

Fuel

The neutron radiography after the 013-irradiation showed a centre void in all central (enriched) pellets, the void diameter being up to about 1½ mm. These pellets also had one or two transverse cracks each, and a few of the pellets showed signs of annular cracks. After ramping (test 050), the centre void appeared slightly thinner along the pellet stack and about 1 mm shorter at the bottom, although the overall shape was unchanged. Transverse fuel cracks were less clear, several had disappeared and a few new cracks could be seen. More pellets now exhibited annular cracks. The limited metallographic examination showed indications of fuel-clad reaction as noted above. Columnar grain growth extended until approximately 50% of the radius. Using the model of Nichols (6), this corresponds to a centre temperature of about 2200 K (1927° C).

The results of the fission gas analysis is shown in Table II. The He content corresponds to a partial He pressure of 0.16 MPa (1.6 ata), compared to a fabrication specification of initial filling gas of 0.1 MPa (1 ata) He. The fabrication records give no reason to believe that the specification was not met. It thus appears that the increase in He contents should be attributed to other sources such as ternary fission and alpha decay of heavy isotopes (in particular ^{242}Cm to ^{238}Pu).

Pins M2-2B and T9-3B (Tests 013, 055 and 067)

Cladding

Similar to M20-1B, the other two pins exhibited various degrees of surface corrosion after the 013-irradiation, with areas near pellet interfaces to some extent more heavily corroded, see

Fig. 4. A metallographic section near a pellet interface is shown in Fig. 5, with oxide nodules almost grown together on the outer clad surface. The maximum nodule thickness seen on M2-2B was 60 µm, associated with a wall thickness reduction of 5-6%. Again, there was no significant change after subsequent irradiation periods.

For M2-2B, the O13-irradiation resulted in irregular diameter decreases up to about 50 µm, the irregularity likely being attributable to a varying extent of corrosion and possibly scaling-off of oxide along the pin; part of it perhaps also to local ovalisation. Many ridges up to 25-50 µm could be seen. The O55-irradiation added little, if any change. As a result of the O67-irradiation, some minor diameter decrease was observed, possibly as a result of scaling-off of surface oxide.

Also for T9-3B, the O13-irradiation gave irregular diameter decreases, locally as large as 100 µm; part of this may be attributed to increased ovality, so that an overall average decrease of some 50 µm would be a reasonable figure. Again it is not clear how much of the diameter variations can be related to corrosion effects. Many ridges up to 25 µm were observed. The O55-irradiation had little, if any effect. After test O67, the diameter was little different at the top end, whereas the mid and bottom parts of the pin had increased by 25-50 µm.

Eddy current testing indicated a variety of ridges and irregularities. Many of the signals could be correlated to ridge positions from profilometry and hydrides (hydrogen pick-up from corrosion) from neutron radiography and metallography. Cross sections at two of the pellet interfaces of M2-2B showed extensive fuel-clad reaction, and also apparent fission-product lumps in the fuel-clad gap. This possibly explains several of the ECT signals, which could not be clearly correlated with specific features from other examinations. No cladding cracks were observed in these two metallographic cross sections.

Fuel

The neutron radiography of M2-2B and T9-3B revealed centre void formation and pellet cracking that were generally similar to the observations for M20-1B, although not all central pellets of M2-2B had a centre void.

The initial metallographic examination of M2-2B revealed extensive fuel-clad reaction, as already noted, in many cases at or near radial pellet cracks. This is illustrated in Fig. 6, which shows partially cracked deposits on the clad ID, with a total thickness up to about 150 µm. The layer nearest the clad is about 5 µm thick and from its appearance believed to be zirconium oxide. Next follows a somewhat thicker, irregular layer, covered by another, thick layer with islands of UO_2 grains. These two layers are probably rich in U and Cs, and the thinner layer also in Zr, as judged from comparison with previously published observations (6). The gap between the layer and the pellet edge is rather uniform, about 25 µm wide (radially), indicating firm fuel-clad contact in the hot condition at this circumferential position. Part of the pellet edge also has a reaction layer which seems to penetrate further into the UO_2 grain boundaries.

A cross section (91 mm above the bottom of the pellet stack) in a pellet with centre void had columnar grain growth up to about 40% of the radius; with Nichols' model (6), this corresponds to a centre temperature around 2100 K (1827° C). The next pellet above had no centre void and no columnar grains, the centre temperature is thus not likely to have exceeded 2000 K (1727° C).

Fission gas analysis results are included in Table II. The He content of both pins corresponds to a partial pressure of 0.14 MPa (1.4 ata), i.e. ternary fission and alpha decay have presumably also here contributed to the He content.

DISCUSSION

Power Ramp Performance

The pre-ramp irradiation and ramp testing is summarized in Table III, with details presented in Table IV. As already noted, all fuel pins remained intact during the entire irradiation. The overpower application of 45 and 43 kW/m (450 and 430 W/cm) at the high burnup was significant as compared to the latest "steady-state" irradiation levels of 31 and 23 kW/m (310 and 230 W/cm). However, the overpower levels did not exceed the maximum power level of 50 KW/m (500 W/cm) experienced early in life.

The pre-ramp irradiation resulted in significant surface corrosion, which makes the evaluation of diameter measurements difficult. With this reservation, the long O13-irradiation produced a diameter reduction generally about 50 µm and formation of many ridges, with heights up to 25-50 µm (diametral). The subsequent irradiations produced only minor changes. It thus appears that the conditioning received by the fuel pins at the high-power operation early in life remained effective to counteract the effects of clad creep-down and fuel swelling during pre-ramp irradiation, as well as fuel expansion and additional swelling during the overpower application.

The integrity of the fuel pins was confirmed by puncturing and gas analysis. Certain ECT signals were indicative of cladding defects, but metallographic examination at two pellet interface positions revealed no cladding cracks. These ECT signals were, therefore, attributed to a combination of surface corrosion, hydriding (pick-up from corrosion) and fuel-clad reaction layers and fission products in the gap, as observed metallographically.

Fission Product Release

The fission gas release was considerable, corresponding to 30-40% as determined after the ramp testing (Table II). Data have been published (8) on gas release after fast ramps to overpower levels of approximately 50 kW/m (400 W/cm). Extrapolation of these data to the power levels used in the present tests would indicate an expected release in the range 10-25%, i.e. somewhat lower than the present results. However, this comparison is tentative only, since details such as fuel pin design, burnup etc. were not given for the data in Ref. (8).

The measured gas release was higher for pin M20-1B than for the other two pins, in agreement with its power history; the heat load was higher both before and during the ramp, whereas the burnups, i.e. the gas inventories, were approximately the same. T9-3B saw heat loads slightly higher than M2-2B and should accordingly have exhibited a slightly higher release fraction. That this was not born out clearly by the experiment is perhaps obscured by the scatter often observed in fission gas release measurements.

The extent of columnar grain growth in two metallographic cross sections in the upper (M2-2B) and middle (M20-1B) pins also agree qualitatively with the calculated heat load levels. The temperatures calculated from the restructuring should be treated with some caution because of the long and varied power history. It is difficult to explain the pronounced difference in fuel structure between the two neighbouring pellets in pin M2-2B.

The gas analyses in Table II indicate a certain He generation during irradiation. Possible He sources are yield from ternary fission and alpha decay of heavy isotopes, notably ^{242}Cm. It has been shown (9) that these two sources can account for the observed increase in He content for pin M2-2B and presumably also for the other two pins.

The limited metallographic examination revealed extensive fuel-clad reaction, in many cases at or near radial pellet cracks. Comparison with published information indicates the presence of significant amounts of fission-product Cs. These reaction layers are probably to a large extent a burnup effect, although the extended hold-time at overpower may have caused additional reaction.

CONCLUSIONS

1. The three pins all survived significant power ramps at burnup levels of 2500 and 2450 GJ/kg U (25,500 and 25,000 MWD/te UO_2). This is attributed to the conditioning received during high-power operation early in life.

2. The fission gas releases were significant: 30-40%. The gas analysis indicated a certain He generation during irradiation; this is attributed to ternary fission yield and alpha decay of ^{242}Cm.

3. Initial metallographic examination revealed extensive fuel-clad reaction, probably to a large extent a result of the long pre-ramp irradiation.

APPENDIX: DETAILS OF IRRADIATION CONDITIONS

The following sections describe the principles used to obtain the irradiation conditions and the results are provided in detail, so that input can be formulated for fuel performance code calculations. This applies to: power history including burnup, fission gas generation, fast neutron flux in cladding, and cladding surface temperature.

Test Average Power History

Continuous measurement of flow rate and temperature increase of the secondary rig cooling water provided the rig thermal output. Subsequent corrections for gamma heat in the rig materials and the nonfissile fuel pin materials (both obtained from measurements in the specific DR 3 positions) gave the fuel thermal output relevant to calculation (of linear heat load and fuel temperature). After a further correction for gamma heat in the fuel, the fission heat output relevant to burnup calculation was obtained.

The gamma scans revealed that Pu build-up occurred faster in the natural end pellets than in the enriched central pellets. As a consequence, the difference between heat generation in the end and central pellets decreased gradually and the ratio approached unity. Calculations (10) adapted to DR 3 conditions of this ratio as a function of burnup were used to separate heat load and burnup for central and end pellets (but still on a test average basis).

Calculations based on calorimetry for the single-pin test 050 would be less accurate because of the relatively large rig gamma heat correction. The power history for pin M20-1B in the 050-irradiation was then obtained as follows. From the EOL-013 calculations and gamma scan on the (shortlived) $^{95}Zr/Nb$ isotopes, the M20-1B fission heat output at EOL-013 was obtained. This was then proportioned with the thermal flux ratio for the DR3 core positions of the tests 050 and EOL-013; adding the fuel gamma heat gave the input to the heat load calculation. The EOL-050 burnup of M20-1B was obtained by adding the 050-increment to the level calculated from the EOL-013 test level and ^{137}Cs gamma scan.

The results of these calculations are presented in Tables IV and V.

Individual Pin Calculations

The above test average data were converted into pin average and local data by means of available gamma scans (^{137}Cs for EOL-013 and EOL-067, $^{140}Ba/La$ for EOL-050) and the physics calculations (10) of the heat generation ratio for end-to-central pellets.

The pin average burnups at the end of each test were obtained from the test average levels by means of the following fractional areas calculated from ^{137}Cs gamma scans (EOL-013, EOL-067):

Test	M2-2B	M20-1B	T9-3B
013	0.3165	0.3533	0.3302
050	-	1	-
055	0.4863	-	0.5136
067	0.4863	-	0.5136

The M20-1B burnup was calculated as described in the previous sections.

Results are included in Table IV.

Comparison of Calorimetric and Radiochemical Burnup Determination

The calorimetric calculations were checked by radiochemical analysis of two samples, taken from pins M20-1B (EOL-050) and M2-2B (EOL-067).

The above calculations provided the local calorimetric burnup values for the two samples. Physics calculations (10) for the specific DR 3 conditions showed that a value of 32 pJ/fission (200 MeV/fission) would give a relevant conversion to % FIMA (fission per initial metal atoms), for comparison with results of the radiochemical ^{148}Nd analysis (11):

Sample	M20-1B-4	M2-2B-5
Calorimetry Radiochemistry	3.28% FIMA 3.45% FIMA	2.88% FIMA 2.87% FIMA
Relative difference	5%	0.3%

The agreement between the results of the two methods is good and shows that the calorimetry is reliable.

Fission Gas Generation

The fission gas quantity generated in each pin was calculated from the above pin average burnup and the value of 32 pJ/fission (200 MeV/fission) together with a generation rate of 0.3 gas atoms/fission. This was then used to calculate the observed fission gas release from the measured gas quantities, see Table II.

Fast Neutron Flux in Cladding

Fast neutron flux levels in the centre of the hollow DR 3 fuel elements were obtained from Ni wire scans. These unperturbed fluxes were then modified by DR 3 physics calculations (12) to give estimates of the fast flux in the fuel pin cladding. The results were as follows:

Test No.	DR 3 Period No.	Fast Flux in Clad $n/m^2/s$	Total Irr. Time Ms (hrs.)	Fast Fluence at Test End n/m^2
013	118-137	4.2×10^{17}	39.91 (11087)	
	139-143	3.5×10^{17}	10.08 (2801)	
	144-158	4.2×10^{17}	28.74 (7994)	3.2×10^{25}
050	169	6.0×10^{17}	1.99 (552)	3.3×10^{25}
055	172-176	3.3×10^{17}	10.24 (2845)	3.7×10^{25}
067	180	6.0×10^{17}	2.40 (667)	3.8×10^{25}

Cladding Surface Temperature

The temperature of the cladding surface depends on the system pressure and the surface heat flux. Above a heat load of approximately 20 kW/m (200 W/cm); there will be boiling on the pin surface at the 7.2 MPa (70 ato) system pressure. The cladding surface temperature is to be calculated from the following expressions:

$$T\ [K] = 554 + 1.45\ (Q[kW/m^2])^{0.25}$$

or $$T\ [^{\circ}C] = 281 + 2.57\ (Q[W/cm^2])^{0.25};$$

this includes an estimated 4 K (4° C) depression of coolant boiling point due to dissolved He.

ACKNOWLEDGEMENT

The achievements presented in this report resulted from the effort of many staff members of the departments of Metallurgy, Engineering, Chemistry, and DR 3 Reactor at Risø. The authors gratefully acknowledge their collaboration throughout the phases of design, fabrication, irradiation, and hot-cell examination, as well as their stimulating discussions and comments during the evaluation of the results.

REFERENCES

1. P. KNUDSEN and K. BRYNDUM, "UO_2-Zr Performance Evaluation in Overpower Testing at 21,000 MWD/MT UO_2", Trans. Am. Nucl. Soc., 19, 140 (1974).

2. P. KNUDSEN, C. BAGGER, and M. FISHLER, "Characterization of PWR Power Ramp Tests", Proc. ANS Topical Meeting on Water Reactor Fuel Performance, May 9-11, 1977, St. Charles (Ill.), pp. 243-252, ANS, La Grange Park (Ill.) (1977).

3. H. H. HAGEN, K. HANSEN, and J. A. LETH, "Design and Experience with Rigs Simulating LWR Conditions in a Research Reactor", IAEA-SM-165/8, International Atomic Energy Agency, Vienna (1972).

4. K. H. HANSEN and J. A. LETH, "Danish High Pressure Irradiation Facilities Used for Overpower Testing of Experimental UO_2-Zr Fuel Pins", Risø-M-1862, Risø National Laboratory (1976).

5. P. KNUDSEN, "Ramp Testing of UO_2-Zr Fuel Pins up to 29,000 MWD/te UO_2", Trans. Am. Nucl. Soc., 27, 244-5 (1977).

6. F. A. NICHOLS, "Theory of Columnar Grain Growth and Central Void Formation in Oxide Fuel Rods", J.Nucl. Mat., 22, 214-222 (1967).

7. J. BAZIN, J. JOUAN, and N. VIGNESOULT, "Les Réactions Oxyde-Gaine et Leur Influence sur le Comportement de la Colonne Combustible des Réacteurs à Eau", Proc. Eur. Nucl. Conf., Paris, 21-25 April 1975, pp. 123-139, Pergamon Press, Oxford (1976).

8. F. GARZAROLLI, R. MANZEL, M. PEEHS, and H. STEHLE, "Observations and Hypothesis on Pellet-Clad Interaction Failures", Kerntechnik, 20, 27-31 (1978).

9. H. CARLSEN, "Xenon, Krypton and Helium Release in High Burn-Up UO_2-Zr Fuel Rods", paper presented at the "Workshop on Fission Gas Behaviour", Karlsruhe, 26-27 Oct. 1978, Organized by the Joint Research Centre of the European Community.

10. F. HØJERUP and T. PETERSEN, Risø, personal communication.

11. N. R. LARSEN, Risø, personal communication.

12. G. K. KRISTIANSEN, Risø, personal communication.

TABLE I

Fuel Pin Design Details

Fuel Pin No.		M2-2B	M20-1B	T9-3B
Pellet				
Diameter	mm	12.63	12.63	12.63
Length (avg.)	mm	12.6	12.3	12.5
Dishing depth* (both ends)	mm	0.29	0.29	0.29
Dishing sphere radius	mm	51.5	51.5	51.5
Dishing shoulder	mm	0.75	0.75	0.75
Surface roughness (OD), Ra	μm	1.3	1.3	1.3
Density	%TD	94.4	94.4	94.4
Enrichment, 8 central pellets	%U235	1.45	1.45	1.45
Enrichment, 2 end pellets	%U235	0.72	0.72	0.72
Grain size (avg.)	μm	25	25	25
H_2O content	ppm	less than 10 (estimate)		
N_2 content	ppm	not determined		
Shaping process		cold-press, sinter, grind		
Sintering temperature	K (°C)	1973 (1700) } all pins		
Sintering time (atm.)	ks (hrs.)	7.2 (2) } (H_2)		
Clad				
Inner diameter	mm	12.85	12.84	12.87
Wall thickness	mm	0.54	0.55	0.56
Surface roughness (ID), Ra	μm	0.9	0.9	0.9
Alloy		Zr-2	Zr-2	Zr-4
Temper		CW-SR	CW-SR	CW-SR
Tensile strength (RT)	MN/m^2	740	740	790
Yield strength (RT)	MN/m^2	550	550	560
Elongation in 2" (RT)	%	22	22	22
Pin				
Pellet-clad gap (diam.)	mm	0.22	0.21	0.24
Total pellet stack	mm	126.0	125.0	126.5
- " -	kg	0.159	0.156	0.158
8 central pellets	mm	100.5	98.8	99.9
- " -	kg	0.125	0.123	0.124
2 end pellets	mm	25.5	26.2	26.6
- " -	kg	0.034	0.033	0.034
End plenum spring, mat.		Inconel (all pins)		
- " - , vol.	mm^3	700	700	700
Washer (between spring and end pellet)		Zr-2 (all pins)		
Washer thickn. (12.4 dia)	mm	1.2	2.2	1.2
Total free volume (cold, as-fab.)	mm^3	2910	3050	3060
Helium filling gas	MPa (ata)	0.1 (1)	0.1 (1)	0.1 (1)

*Central pellets only.

TABLE II

Fission Gas Analysis

Pin No.		M20-1B	M2-2B	T9-3B
Total gas content, cm^3 at 0.1 MPa, 293 K (1 ata, 20°C)		56.4	43.3	44.8
Free volume, post-irr., cm^3		2.78	3.07	3.08
Calculated internal pressure MPa at 293 K (ata at 20°C)		2.06 (20.3)	1.43 (14.1)	1.49 (14.7)
Gas composition, vol. %	H_2	(ND)	(ND)	(ND)
	He	7.8	10.2	9.4
	D_2	(ND)	(ND)	(ND)
	N_2+CO	1.1	1.45	0.54
	O_2	0.08	0.08	0.06
	Ar	0.007	(ND)	0.003
	CO_2	0.03	0.35	0.33
	Kr-83	0.45	0.53	0.48
	Kr-84	2.6	2.4	2.6
	Kr-85	0.39	0.37	0.37
	Kr-86	3.2	3.5	3.5
	Xe-130	0.38	0.28	0.34
	Xe-131	5.7	5.7	5.3
	Xe-132	19.0	17.1	18.2
	Xe-134	22.7	21.7	22.0
	Xe-136	36.6	36.4	36.9
	Sum	100.037	100.06	100.023
	Kr	6.64	6.80	6.95
	Xe	84.38	81.18	82.74
	Kr+Xe	91.02	87.98	89.69
Calculated fission gas release, % (see Appendix)		38.9	29.5	29.6

TABLE III

Summary of Irradiation Histories

Test No.	Fuel Pin No.	Test Avg. Heat Load kW/m (W/cm)	Test Duration	Test Avg. Burnup at End of Test GJ/kgU (MWD/teUO$_2$)
013 Pre-ramp	M2-2B M20-1B T9-3B	50 (500) (early max) 31 (310) (end of test)	95 Ms (3 years)	2330 (23,800)
050 Ramp (a)	M20-1B	45 (450)	2 Ms (550 hrs)	2580 (26,300)
055 Re-preramp	M2-2B T9-3B	23 (230)	10 Ms (4 months)	2450 (25,000)
067 Ramp (a)	M2-2B T9-3B	43 (430)	2.4 Ms (670 hrs)	2540 (25,900)

[a] Ramp rate: 35 W/m·s (21 W/cm.min.); no failure indication.

TABLE IVa

Detailed Power History, Test 013

(See also notes at bottom of TABLE IVd)

Per. No	Time h	Test.Avg. P W/cm	Test.Avg. BU MWD/te UO_2	Pin M2-2R Pin Avg. P W/cm	Pin M2-2R Pin Avg. BU MWD/te UO_2	Pin M2-2R 9 P W/cm	Pin M2-2R 10 P W/cm	Pin M2-2R 11 P W/cm	Pin M2-2R 12 P W/cm
118	725	442	1029	420	969	292	470	435	268
119	392	457	1605	434	1511	333	479	448	309
120	566	457	2436	434	2294	347	475	445	323
121	565	497	3341	472	3146	391	513	480	364
122	561	484	4215	460	3969	391	496	465	364
123	557	444	5010	422	4717	366	453	424	341
124	561	455	5830	432	5489	382	463	434	355
125	544	431	6582	409	6197	367	437	410	341
126	563	415	7330	394	6901	357	420	393	332
127	560	405	8056	385	7585	351	408	382	326
128	565	375	8732	356	8222	329	379	355	306
129	550	338	9322	321	8777	299	340	319	278
130	558	373	9986	354	9402	332	375	351	308
131	562	367	10643	349	10021	329	369	346	306
132	560	336	11240	319	10583	302	337	315	281
133	561	333	11833	317	11141	302	334	313	281
134	463	328	12315	312	1159[illegible]	298	328	307	277
135	564	330	12905	314	12151	301	330	309	280
136	559	341	13509	324	12719	313	340	319	291
137	552	344	14113	327	13288	316	342	321	294
139	557	294	14633	279	13778	271	292	274	252
140	562	265	15104	252	14221	245	284	248	228
141	561	254	15554	242	14645	236	253	237	220
142	561	252	16000	240	15065	234	250	235	218
143	560	265	16470	252	15507	247	263	247	230
144	394	325	16875	309	15888	305	323	303	284
145	556	314	17428	299	16409	296	312	293	275
146	556	299	17952	284	16902	281	295	277	262
147	556	301	18481	286	17401	285	298	280	265
148	556	280	18970	266	17861	265	277	260	247
149	560	288	19478	274	18339	274	285	267	255
151	562	301	20012	286	18842	287	297	279	267
152	732	238	20554	226	19352	227	235	220	212
153	723	285	21202	271	19962	274	283	264	255
154	559	272	21680	259	20413	261	268	251	243
155	557	299	22206	284	20908	287	294	276	268
156	554	299	22728	284	21399	288	294	276	268
157	562	299	23258	284	21898	283	294	276	269
158	557	312	23804	297	22415	302	307	288	281

Per. No	Pin M20-1R Pin Avg. P W/cm	Pin M20-1R Pin Avg. BU MWD/te UO_2	Pin M20-1R 5-8 P W/cm	Pin M20-1R 6-7 P W/cm	Pin T9-3B Pin Avg. P W/cm	Pin T9-3B Pin Avg. BU MWD/te UO_2	Pin T9-3B 1 P W/cm	Pin T9-3B 2 P W/cm	Pin T9-3B 3 P W/cm	Pin T9-3B 4 P W/cm
118	471	1102	317	507	436	1017	285	460	489	305
119	487	1719	362	517	451	1587	325	468	498	348
120	487	2609	378	513	451	2408	339	465	494	363
121	529	3579	427	554	490	3303	382	502	514	489
122	515	4515	426	536	477	4167	382	486	517	480
123	473	5367	399	489	438	4952	358	444	472	381
124	484	6245	416	500	449	57[illegible]	372	453	482	399
125	459	7051	399	472	425	6506	358	428	455	383
126	442	7852	389	453	409	7246	348	411	437	373
127	431	8630	382	441	399	7963	341	399	425	367
128	399	9354	359	409	370	8632	322	371	394	344
129	360	9986	326	367	333	9215	292	333	354	313
130	397	10697	361	404	368	9871	324	367	390	347
131	391	11401	358	398	362	10521	321	361	384	344
132	357	12040	329	363	331	11111	295	329	350	316
133	354	12676	328	360	328	11697	295	327	347	315
134	349	13192	324	351	323	12174	291	321	341	312
135	351	13824	328	356	325	12757	294	323	343	315
136	363	14471	341	367	336	13354	305	333	354	327
137	366	15118	344	369	339	13951	309	335	356	331
139	313	15675	295	315	290	14465	264	286	304	283
140	282	16179	267	285	261	14930	240	258	275	256
141	270	16662	257	273	250	15375	231	248	263	247
142	268	17139	255	270	249	15816	229	245	260	245
143	282	17643	269	284	261	16281	241	257	274	258
144	346	18077	332	348	320	16681	298	316	336	319
145	334	18669	322	337	310	17228	289	305	325	309
146	318	19230	306	318	295	17746	275	289	307	294
147	320	19797	310	322	297	18269	278	292	310	298
148	298	20321	289	298	276	18752	259	271	288	277
149	306	20865	298	307	284	19254	267	279	296	286
151	320	21437	312	321	297	19782	280	291	309	300
152	253	22018	247	253	235	20318	222	230	244	237
153	303	22712	298	304	281	20950	267	276	293	286
154	289	23224	284	289	260	21431	259	262	279	273
155	318	23787	313	317	295	21951	281	288	306	300
156	318	24346	314	317	295	22467	282	288	306	301
157	318	24914	315	317	295	22991	282	288	306	302
158	332	25503	329	331	308	23534	295	301	319	316

TABLE IVb

Detailed Power History, Test 050

Per.	Time	Test Avg.		Pin M20-1B			
				5	6	7	8
		P	BU	P	P	P	P
	h	W/cm	MWd/te UO_2	W/cm	W/cm	W/cm	W/cm
169	552	451	26288	484	476	425	420

Note: Test Average = Pin Average

TABLE IVc

Detailed Power History, Test 055

Per.	Time	Test Avg.		Pin M2-2B						Pin T9-3B					
				Pin Avg.		9	10	11	12	Pin Avg.		1	2	3	4
		P	BU	P	BU	P	P	P	P	P	BU	P	P	P	P
	h	W/cm	MWd/te UO_2	W/cm	MWd/te UO_2	W/cm	W/cm	W/cm	W/cm	W/cm	MWd/te UO_2	W/cm	W/cm	W/cm	W/cm
172	522	230	23353	224	22739	238	241	210	204	236	24353	225	229	244	241
173	550	230	23751	224	23127	238	241	210	204	236	24479	225	229	244	242
174	520	238	24141	232	23507	247	249	217	211	244	24881	233	237	252	250
175	559	223	24533	218	23888	230	232	203	198	228	25285	218	221	235	234
176	694	227	25028	222	24370	235	236	207	202	232	25795	222	225	240	239

Table IVd

Detailed Power History, Test 067

Per	Time	Test Avg.		Pin M2-2B						Pin T9-3B					
				Pin Avg.		9	10	11	12	Pin Avg.		1	2	3	4
		P	BU	P	BU	P	P	P	P	P	BU	P	P	P	P
	h	W/cm	MWd/te UO_2	W/cm	MWd/te UO_2	W/cm	W/cm	W/cm	W/cm	W/cm	MWd/te UO_2	W/cm	W/cm	W/cm	W/
180	667	427	25920	417	25239	446	446	390	384	437	26714	421	424	452	453

Notes for TABLE IV:

(i) The heat rating P is composed of P [fiss], representing the heat originating from fissions in the fuel, and P [γ, fuel] representing the heat originating from absorption in the fuel of radiation from the external gamma field.
P [fiss] is determined by subtracting from P the term $Q[\gamma,\ \text{fuel}] \times \frac{\text{fuel weight}}{\text{fuel length}}$.
Q [γ,fuel] (W/g) is given in table IVe. The fuel weight and the fuel length apply to the fuel section in question and are found from table I.

(ii) The local positions (1-12) refer to the axial locations shown on the sketch below of the gamma activity distribution.

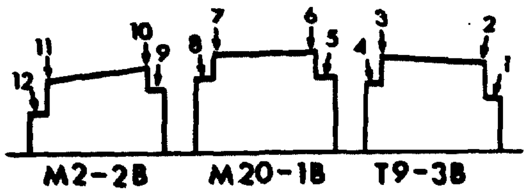

(iii) Conversion factors: 1 W/cm = 0.1 kW/m; 1 MWD/te UO_2 = 0.0982 GJ/kg U.

TABLE IVe

Heat Production in the Fuel Caused by the External Gamma Field

Per.	118-137	139-143	144-158	169	172-176	180
$Q[\gamma,\ \text{fuel}]$ kW/kg	1.22	1.03	1.22	1.93	0.95	1.93

TABLE Va

Power Ramp, Test 050

Test Average Heat Load

Time, min.	0	9-11	12-16	22-36	41-50	58-67	73-93	94+
P[avg.],W/cm	0	43	146	237	263	305	433	451

Notes: (i) Pin avg. heat load identical to test avg. heat load (1 pin only).

(ii) Pin local heat load at each time is obtained by proportioning [P avg.] in this table with data from table IVb. $P[pos.x]_{Ramp} = P[avg.]_{Ramp} \cdot \left(\frac{P[pos.x]}{P[avg.]}\right)_{Table\ IVb}$

(iii) 1 W/cm = 0.1 kW/m.

TABLE Vb

Power Ramp, Test 067

Test Average Heat Load

Time, min.	0	20-27	29-37	38-52	54-70	78+
P[avg.] W/cm.	0	143	192	220	248	427

Notes for Table Vb: (i) Pin avg. heat load = P[avg.] x area fraction ^{137}Cs scan, EOL 067.
The area fraction is given in section: Individual Pin Calculations.

(ii) Pin local heat load at each time is obtained by proportioning P[avg.] in this table with data from table IVd.

$$P[\text{Pos.x}]_{\text{Ramp}} = P[\text{avg.}]_{\text{Ramp}} \cdot \left(\frac{P[\text{Pos.x}]}{P[\text{Test avg.}]}\right)_{\text{Table IVd}}$$

(iii) 1 W/cm = 0.1 kW/m.

List of Figure Captions

List of Tables

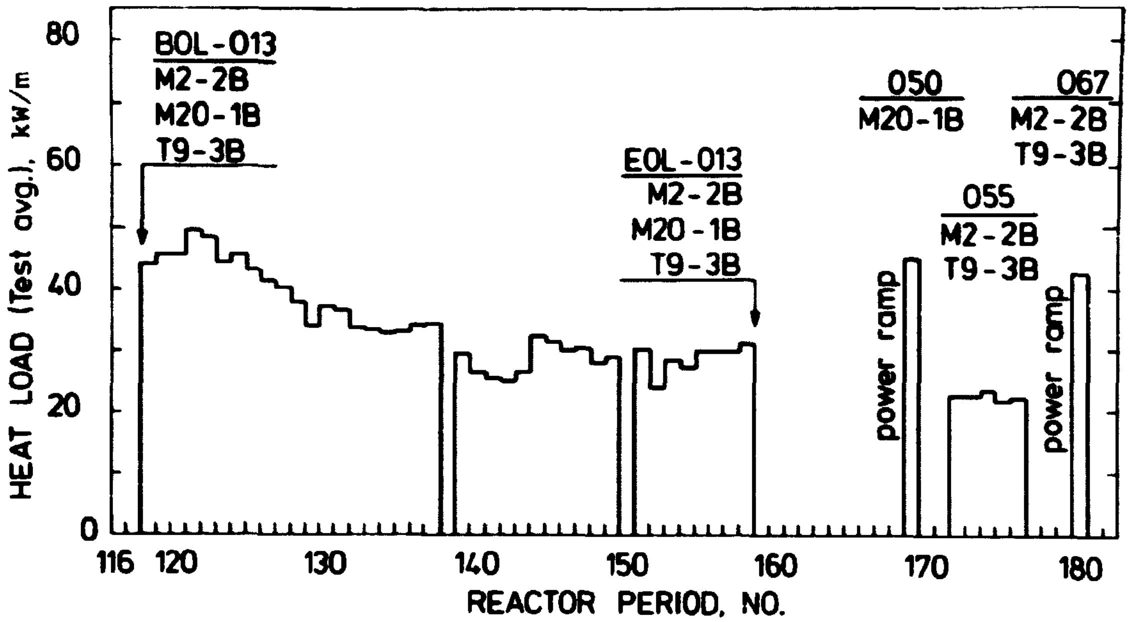

Fig. 1. Summary of Irradiation Histories

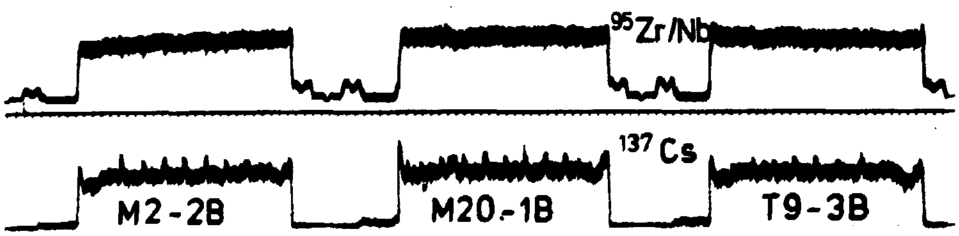

Fig. 2. Gamma Scans after Test 013

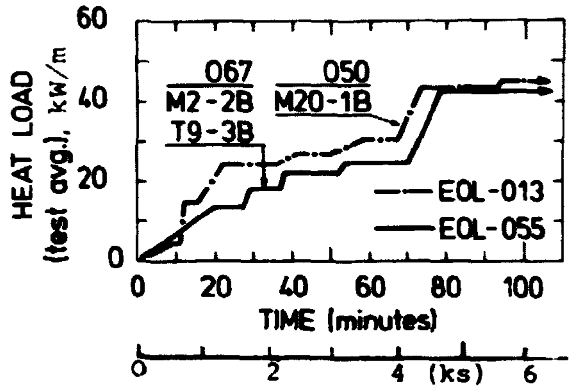

Fig. 3. Power Ramps

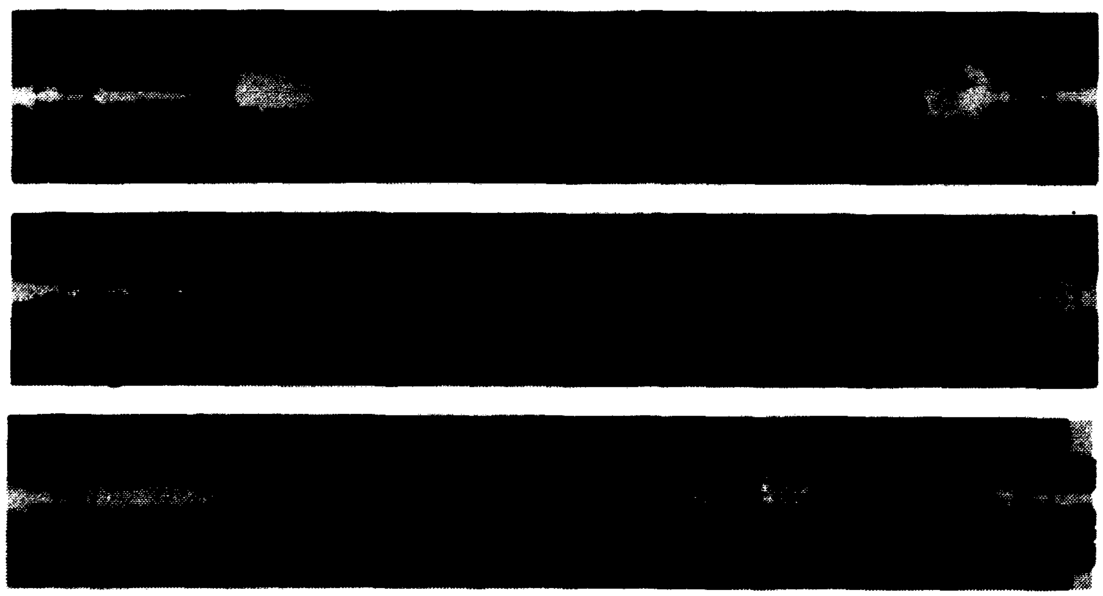

Fig. 4. Cladding Surface Appearance after Test 013 (Pin Sequence from Top: M2-2B, M20-1B, T9-3B); Pin Top Ends to the Left).

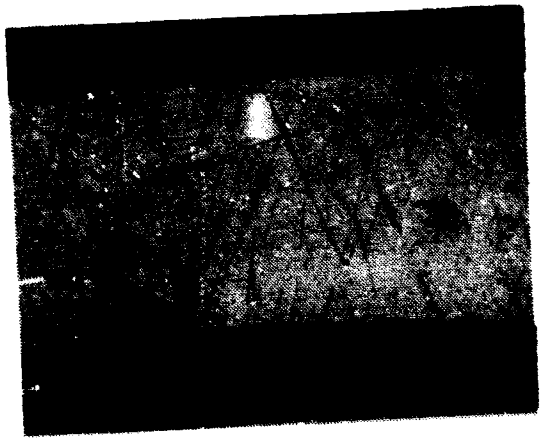

Fig. 5. Nodular Corrosion of Cladding Surface of Pin M2-2B.

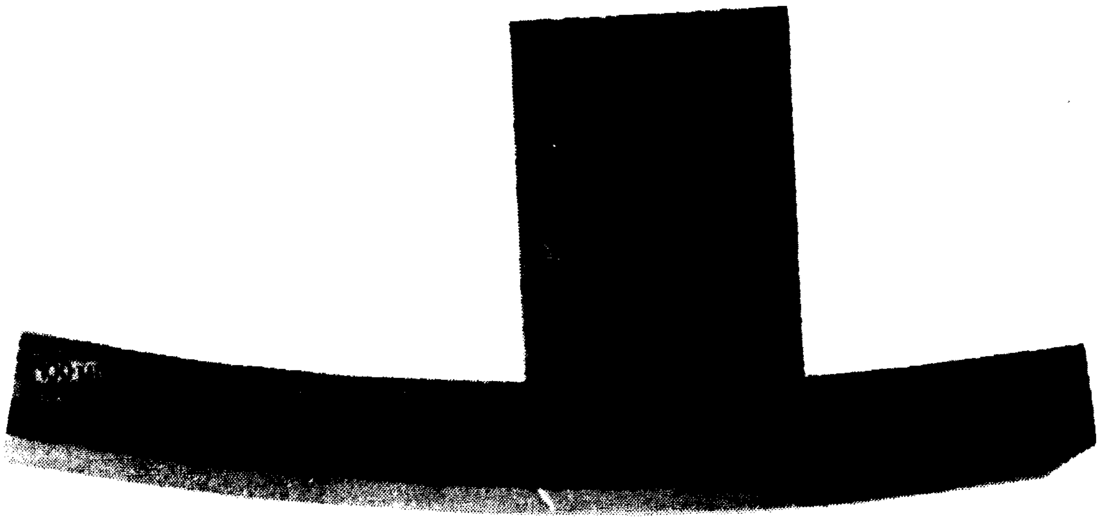

Fig. 6. Fuel-Clad Reaction Layers in Pin M2-2B